Characterization of Hydrous Species in Minerals by High-Speed ^1H MAS–NMR

James P. Yesinowski,*† Hellmut Eckert,†,§ and George R. Rossman‡

Contribution from the Division of Chemistry and Chemical Engineering, California Institute of Technology, Pasadena, California 91125, and Contribution No. 4497 from the Division of Geological and Planetary Sciences, California Institute of Technology, Pasadena, California 91125. *Received August 19, 1987*

Abstract: Proton magic-angle spinning (MAS) NMR at 200 and 500 MHz and at high spinning speeds (ca. 8 kHz) has been used to characterize hydrous species, both stoichiometric and nonstoichiometric, in a variety of minerals. High-resolution ^1H MAS–NMR spectra of minerals containing stoichiometric hydroxyl groups as the only hydrous species are obtainable provided that the hydrogen density in the sample is less than about 15 atoms/nm^3. Structurally isolated water molecules in analcite, $NaAlSi_2O_6 \cdot H_2O$, and gypsum, $CaSO_4 \cdot 2H_2O$, yield characteristic ^1H MAS–NMR spectra with numerous spinning sidebands extending over a range of about 100 kHz, reflecting the strong, largely inhomogeneous character of the homonuclear dipolar coupling. The field dependence of both line widths and spinning sideband patterns provides evidence about the nature of the broadening interactions. Lawsonite and hemimorphite, minerals containing stoichiometric amounts of both OH and H_2O groups, yield spectra with numerous intense spinning sidebands; strong dipolar interactions preclude discrimination of OH and H_2O. Nonstoichiometric hydrogen in nominally anhydrous minerals (feldspars, nepheline, quartz, and grossular garnet) is found to occur in a variety of forms: mobile H_2O in fluid inclusions, anisotropically constrained, isolated H_2O molecules, and clustered species consistent with $H_4O_4^{4-}$ groups in a hydrogarnet substitution.

Water is the dominant low density fluid in the earth's crust, where it plays a crucial role as solvent, transport agent, reactant, and catalyst in the formation and transformation of minerals. In particular, trace amounts of water in nominally anhydrous minerals can have a dramatic influence upon physical and chemical processes and properties.[1] The interaction of water with inorganic solids is also important in materials science, in such areas as ceramics, glasses, catalysts, superconductors, piezoelectrics, and fiber optics.

Oxygen-bound hydrogen species in minerals can occur in many different forms. They can occur as part of the crystal structure in the form of stoichiometric OH groups, water molecules, and hydronium ions. Hydroxyl groups can also occur as part of a simple substitution (e.g., OH^- for F^-), a coupled substitution (e.g., $Al^{3+} + H^+$ for Si^{4+}), or the classical hydrogarnet substitution ($H_4O_4^{4-}$ for SiO_4^{4-}).[2] Water molecules can occupy vacant cation and anion sites, zeolitic sites, or interlayer regions. Water molecules can also be present on the mineral surface, in microscopic cracks in the crystal, or in macroscopic fluid inclusions.

Although diffraction techniques are generally able to elucidate the forms and sites in which hydrogen occurs in compounds containing stoichiometric amounts of hydrogen, these techniques generally do not provide such information for minerals with low levels of nonstoichiometric hydrogen. In these cases, spectroscopic approaches hold more promise. Infrared spectroscopy is indeed useful in distinguishing qualitatively between different sites;[3] however, peak assignments suffer from numerous uncertainties, and the difficulty of obtaining reliable extinction coefficients limits the ability to obtain quantitative information.

Proton nuclear magnetic resonance spectroscopy is a promising technique for addressing these problems, since it is a sensitive probe of solely the hydrogen environment and is inherently quantitative. NMR spectra in the solid state are usually very broad due to the strong anisotropic interactions present. However, high resolution spectra of solids can frequently be obtained by spinning the sample rapidly about an axis making the "magic angle" of 54.7° with respect to the magnetic field (MAS–NMR).[4] The effect of such spinning upon the NMR spectrum depends upon the type and the strength of the broadening mechanisms relative to the spinning frequency. The two basic types of broadening mechanisms in MAS NMR are homogeneous interactions arising from homonuclear dipole–dipole couplings and inhomogeneous interactions such as heteronuclear dipole–dipole coupling, chemical shift anisotropy, and nuclear electric quadrupole coupling.[5] If the static line shape is dominated by inhomogeneous interactions, magic angle spinning will result in a sharp central line at the isotropic chemical shift as well as "spinning sidebands" spaced at integer multiples of the spinning frequencies. The envelope of this spinning sideband pattern approximates the static powder spectrum, especially in the limit of low spinning speeds. In contrast, homogeneous interactions do not give rise to well-resolved spinning sidebands unless the spinning frequency is comparable to the strength of the interactions; even higher spinning frequencies are required to obtain very narrow central peaks.

The main problem generally encountered in ^1H magic angle spinning NMR is the strength of the homogeneous dipolar interactions among protons, which renders it difficult to achieve significant line-narrowing at technically feasible spinning speeds. However, in minerals with low hydrogen contents, where the hydrogen-bearing species are relatively isolated from each other, inhomogeneous line-broadening mechanisms dominate. For instance, it has been shown theoretically that in the special case of an isolated two-spin system (e.g., in structurally isolated water molecules) the character of the homonuclear dipolar interaction between the two protons is inhomogeneous.[5] We have recently demonstrated this effect in a number of crystalline hydrates, which yield high-resolution ^1H MAS–NMR spectra with numerous intense spinning sidebands.[6,7]

High-speed ^1H MAS–NMR should be extremely useful for the analysis of hydrous species in minerals. NMR experiments under the appropriate experimental conditions are inherently quantitative: both the relative amounts of various resolved species within a given sample as well as the total absolute hydrogen content can be

* Author to whom correspondence should be addressed.
† Division of Chemistry and Chemical Engineering.
§ Current address: Department of Chemistry, University of California, Santa Barbara, Goleta, California 93106.
‡ Division of Geological and Planetary Sciences.

(1) Fyfe, W. S.; Price, N. J.; Thompson, A. B. *Fluids in the Earth's Crust, Developments in Geochemistry*; Elsevier Scientific: New York 1978; p 1.
(2) Foreman, D. W., Jr. *J. Chem. Phys.* **1968**, *48*, 3037.
(3) Aines, R. D.; Rossman, G. R. *J. Geophys. Res.* **1986**, *89*, 4059.
(4) Andrew, E. R.; Bradbury, A.; Eades, R. G. *Nature (London)* **1959**, *183*, 1802. Lowe, I. J. *Phys. Rev. Lett.* **1959**, *2*, 285.
(5) Maricq, M. M.; Waugh, J. S. *J. Chem. Phys.* **1979**, *70*, 3300.
(6) Yesinowski, J. P.; Eckert, H.; Rossman, G. R. *Abstracts with Programs*; International Mineralogical Association, 14th General Meeting, Stanford, CA, 1986; p 275.
(7) Yesinowski, J. P.; Eckert, H. *J. Am. Chem. Soc.* **1987**, *109*, 6274.

0002-7863/88/1510-1367$01.50/0

Table I. Compositional Formulas, Localities, and ^1H MAS-NMR Parameters of the Minerals Studied

mineral name	compstnl formula	origin[a]	δ_{iso} (^1H),[b,c] ppm	d(O–H···O),[d] ppm	$\Delta\nu_{1/2}$, Hz (MAS-NMR) 200 MHz	500 MHz	C_H, nm^{-3}	cryst struct ref
pyrophyllite	$Al_2Si_4O_{10}(OH)_2$	Mariposa Co., CA	2.3	301	850	770	9.5	15
talc	$Mg_3Si_4O_{10}(OH)_2$	CA	1.1	306	1260	2550	8.9	32
tremolite	$Ca_2Mg_5Si_8O_{22}(OH)_2$	unknown	0.7	307	320	490	4.5	34
topaz	$Al_2SiO_4[F_{0.98}(OH)_{0.02}]_2$	Minas Gerais, 0.7 wt% OH	3.0	298	690		0.5	42
elbaite	$Na(Li,Al)_3Al_6(BO_3)_3$-$Si_6O_{18}(OH,F)_4$	Himalaya mine	4.7	292				33
			2.8	299	two overlapping peaks			
datolite	$CaBSiO_4(OH)$	Great Notch, NJ	4.3	293 (321)	1,270	1,350	11.3	35
diaspore	AlOOH	Chester, MA	nd[e]		no narrowing obsd		33.9	39
pectolite	$NaCa_2Si_3O_8(OH)$	Asbestos, Canada	15.8	248 (247)	780	710	5.2	16
analcite	$NaAlSi_2O_6\cdot H_2O$	Golden, CO	3.1	298 (341)	1270		13.2	20, 21
gypsum	$CaSO_4\cdot 2H_2O$	Lake Mead, NV	5.3	(281, 288)	3200		32.4	40, 41
colemanite	$CaB_3O_4(OH)_3\cdot H_2O$	Ryan, Death Valley, CA	nd[e]		no narrowing obsd		35.4	31
hemimorphite	$Zn_4Si_2O_7(OH)_2\cdot H_2O$	unknown	3.6 ± 1.5	296 (294, 313)	2200	2600	17.4	26
lawsonite	$CaAl_2Si_2O_7(OH)_2\cdot H_2O$	Marin Co., CA	nd[e]	(267)	3300	4500	23.7	24, 25
microcline	$KAlSi_3O_8$	amazonite pegmatite, Lake George, CO, 0.11 (0.11) wt % H_2O	4.6 (100%)[f]	292	*f*	*f*		36
		Elizabeth R. pegmatite, Ramona, CA, 0.10 (0.11) wt % H_2O	5.0 (4%)[f]	290	*f*	*f*		
			4.6 (96%)	292				
		White Queen pegmatite, Pala, CA 0.14 (0.14) wt% H_2O	5.0 (3%)[f]	290	*f*	*f*		
			4.6 (97%)	292				
buddingtonite	$((NH_4),K)AlSi_3O_8$	Sharon Heights Locality, Menlo Park, CA	6.8					
nepheline	$(Na,K)AlSiO_4$	Ontario, Canada, 0.36 (0.27) wt.% H_2O	4.6 (26%)[f]	292	*f*	*f*		37, 38
			4.6 / 3.4 (74%)	292 / 297	overlapping components			
quartz	SiO_2	Coleman Mines, Hot Springs, AR, 0.07 (0.07) wt% H_2O	4.8 (100%)[f]	291	*f*	*f*		43
grossular	$Ca_3Al_2(SiO_4)_3$	Transvaal, South Africa, 3.6 wt% H_2O	nd[e]		narrowing by MAS not sufficient		7.1	

[a] Water contents from H_2 manometry or TGA are included; numbers in parentheses give water contents by NMR quantitation. [b] ±0.1 ppm versus TMS. [c] The fractional areas of peaks are given by the numbers in parentheses. These fractional areas were determined by fitting the spectra at 200.27 MHz to Lorentzian peaks by using the Nicolet NMRCAP routine. [d] Numbers in parentheses give values from diffraction data. [e] nd = not determined. [f] Fluid inclusions, line widths determined by field inhomogeneity.

determined. The range of isotropic chemical shifts for oxygen-bound hydrogen in solids is quite large (ca. 20 ppm), and the shifts correlate well with the strength of hydrogen bonding.[8] The intensities of the spinning sidebands are related to the anisotropic interactions present[9] and hence carry structural as well as dynamical information. The motional state of a given species is important in the identification and discrimination of structural hydrate water, liquid inclusions, and surface-adsorbed species.

In this paper we report the characterization of hydrogen-bearing minerals using ^1H MAS-NMR at both 200 and 500 MHz and at spinning speeds of up to 8.8 kHz. Minerals containing stoichiometric quantities of hydrogen provide the benchmark data needed to address the distribution of nonstoichiometric and trace amounts of hydrogen in minerals. Results are presented for feldspars, quartz, nepheline, and grossular garnet to demonstrate the usefulness of the method in distinguishing various hydrogen environments in these nominally anhydrous minerals.

Experimental Section

Sample Origin and Characterization. Samples in the present study were either taken from the mineral collection of the Division of Geological and Planetary Sciences at the California Institute of Technology or are portions of previously described specimens (ref 24, 45, and 51 of the Discussion section for the lawsonite, feldspar, and grossular garnet samples, respectively). Their origins, characteristics, and chemical compositions are summarized in Table I. Topaz, elbaite, hemimorphite, gypsum, datolite, colemanite, and pectolite were obtained as large single crystals or clusters of crystals, and their identity was confirmed by crystal morphology. The identity of tremolite was confirmed by electron probe microanalysis and that of analcite and talc by X-ray powder diffraction. A Nicolet 60 SX FTIR spectrometer was used to obtain the spectra of feldspars reported in this paper as well as to confirm the identity of the talc, quartz, and nepheline samples. The samples were coarsely ground in mullite or boron carbide mortars.

NMR Studies. The NMR studies were carried out at two different field strengths. The 200 MHz ^1H NMR spectra were obtained by using a homebuilt spectrometer described previously,[10] and the 500 MHz spectra were obtained on a Bruker WM-500 spectrometer. Both spectrometers were equipped with ^1H MAS-NMR probes from Doty Scientific that were specially designed to have a low proton background signal. A sharp ^1H MAS-NMR peak at 1.5 ppm was observed for empty spinning rotors. This signal could be greatly reduced by washing the rotors with hexane and handling them with latex gloves, suggesting that it arises from the methylene chains of skin lipids. In some cases, this peak appeared to arise from organic contamination of the sample, since it could be eliminated by refluxing the sample with CCl_4. Therefore, any sharp peaks at 1.5 ppm in samples containing *low* levels of hydrogen were attributed to organic contamination. A 5-mm nonspinning tube of ethanol was used to optimize the field homogeneity and to reference the hydroxyl chemical shift in hydroxyapatite (0.2 ppm versus TMS).[7] The hydroxyapatite sample was subsequently used as a secondary chemical shift reference in order to improve the reproducibility of the chemical shift measurements (±0.1 ppm). Measurements were carried out by using variable spinning speeds up to a maximum of ca. 8 kHz. The ^1H 90° pulse lengths were 2 μs at 200 MHz and 8 μs at 500 MHz. Spin-lattice relaxation times, measured by the inversion recovery method, range from less than 10 ms in lawsonite to ca. 10 s for the structural water component in the feldspars. Quantitative MAS-NMR spectra were readily obtained under nonsaturating conditions. For the feldspar, quartz, and nepheline samples, the absolute water contents were determined by integration of the ^1H MAS-NMR spectra and subtraction of the integrated area arising from the probe background. As a standard for absolute quantitation, a spinning sample of pyrophyllite ($Al_2Si_4O_{10}(OH)_2$), analyzed by hydrogen manometry to contain 5.0 wt.% H_2O, was used. The water contents thus determined by NMR are compared in Table I with the results obtained by traditional methods.

All free induction decays were multiplied by an exponential apodization function equivalent to a 10–20 Hz linebroadening. All line widths reported in Table I were measured as full width at half-height. The curved base line apparent in some spectra arises from delayed receiver recovery; no base line correction was applied due to the subjective nature of such corrections.

(8) Berglund, B.; Vaughan, R. W. *J. Chem. Phys.* **1980**, *73*, 2037.

(9) Herzfeld, J.; Berger, A. E. *J. Chem. Phys.* **1980**, *73*, 6021.

(10) Eckert, H.; Yesinowski, J. P.; Sandman, D. J.; Velazquez, C. S. *J. Am. Chem. Soc.* **1987**, *109*, 761.

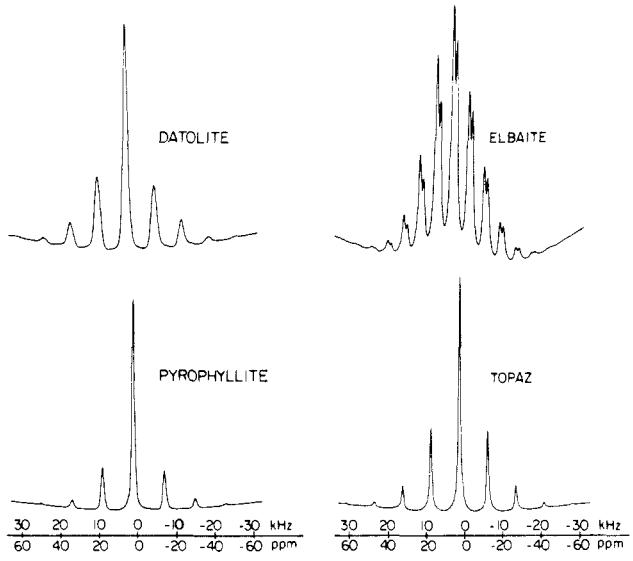

Figure 1. ^{1}H MAS-NMR spectra at 500.13 MHz of compounds containing structural hydroxyl groups: (a) datolite, spinning speed 7.1 kHz; (b) pyrophyllite, spinning speed 8.0 kHz; (c) elbaite, spinning speed 4.1 kHz; (d) topaz, spinning speed 7.3 kHz.

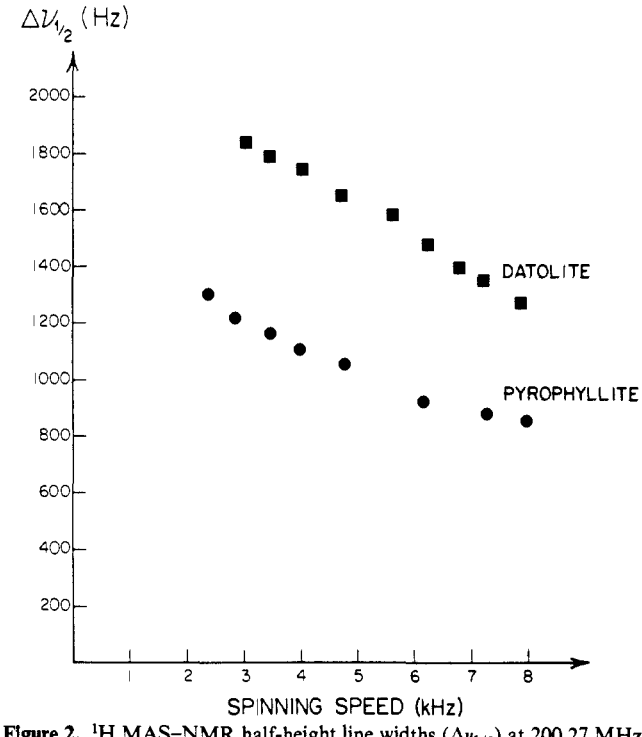

Figure 2. ^{1}H MAS-NMR half-height line widths ($\Delta\nu_{1/2}$) at 200.27 MHz of the OH center peaks in pyrophyllite and datolite versus spinning speed.

Results

We investigated three groups of mineral samples in which the hydrogen is present in a well-defined chemical form: (1) compounds containing hydrogen exclusively in the form of OH groups, (2) compounds containing hydrogen only in the form of molecular H_2O, and (3) compounds containing both species. The ^{1}H isotropic chemical shifts (versus TMS) and MAS-NMR centerband line widths measured for these compounds are listed in Table I. The line widths were measured at spinning speeds between 7.1 and 8.8 kHz. For a given sample, the differences in the spinning speeds at the two different fields were kept as small as possible and never exceeded 1 kHz. The 500.13 MHz ^{1}H MAS-NMR spectra of several compounds containing only OH groups are shown in Figure 1. In addition to the central peak located at the isotropic chemical shift, three to four pairs of spinning sidebands are observed at 7–8 kHz spinning speeds. In elbaite (Figure 1c), two well-resolved,

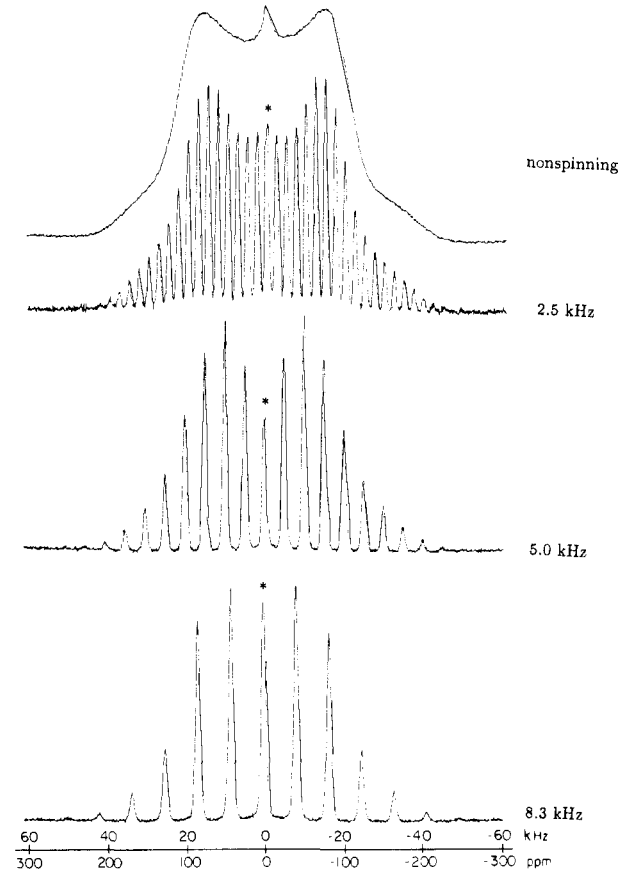

Figure 3. ^{1}H MAS-NMR spectra at 200.27 MHz of analcite, $NaAlSi_2O_6 \cdot H_2O$, at indicated spinning speeds. The centerbands are indicated by asterisks.

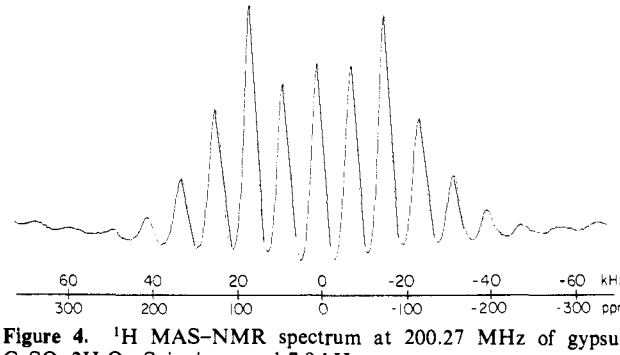

Figure 4. ^{1}H MAS-NMR spectrum at 200.27 MHz of gypsum, $CaSO_4 \cdot 2H_2O$. Spinning speed 7.9 kHz.

chemically distinct OH sites are observed. Figure 2 shows the dependence of the 200.27 MHz ^{1}H MAS-NMR centerband line width on the spinning speed for the minerals pyrophyllite and datolite and demonstrates a gradual narrowing of the lines at higher spinning speeds. Figures 3 and 4 show the ^{1}H MAS-NMR spectra of analcite and gypsum, both of which contain hydrogen only in the form of H_2O groups. Very distinctive spinning sideband patterns extending over a wide frequency range are observed for these compounds. The ^{1}H MAS-NMR spectra of hemimorphite and lawsonite, both of which contain stoichiometric amounts of H_2O and OH groups, are shown in Figure 5. The minor sharp component in Figure 5b is assigned to water in fluid inclusions or surface water, since rapid pulsing experiments revealed a large difference in T_1 values and hence an absence of spin diffusion between this component and the major broader signal.

Figures 7–9 and Figures 11 and 12 show ^{1}H MAS-NMR spectra of minerals containing nonstoichiometric hydrogen. Three feldspars, whose infrared spectra are shown in Figure 6, were investigated. The 500.13 MHz ^{1}H MAS-NMR spectra of these samples are shown in Figure 7 and, in an expanded view, Figure 8. Inversion recovery spectra of one of these feldspar samples are

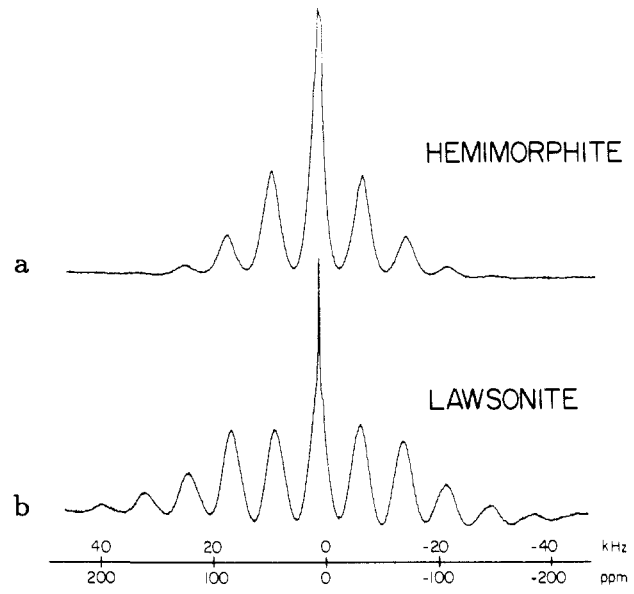

Figure 5. ^1H MAS-NMR spectra at 200.27 MHz of minerals containing both structural OH and H_2O groups: (a) hemimorphite, $Zn_4Si_2O_7(OH)_2 \cdot H_2O$; spinning speed 8.0 kHz; (b) lawsonite, $CaAl_2Si_2O_7(OH)_2 \cdot H_2O$; spinning speed 7.8 kHz.

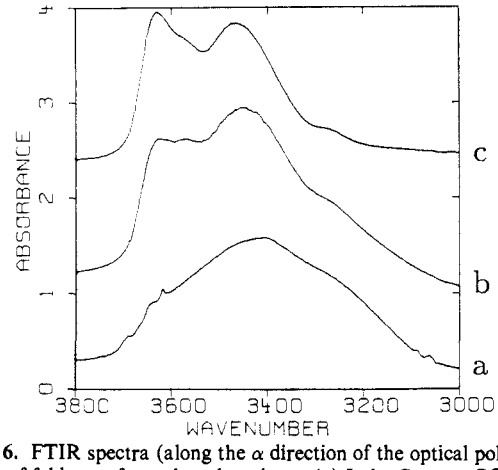

Figure 6. FTIR spectra (along the α direction of the optical polarization tensor) of feldspars from three locations: (a) Lake George, CO, plotted as 5.0 mm thick; (b) Elizabeth R Mine, 0.50 mm thick; (c) White Queen Mine; 0.50 mm thick.

shown in Figure 9. Figures 10 and 11 display IR and NMR spectra, respectively, of nepheline containing nonstoichiometric hydrogen. Figure 12 shows the ^1H MAS-NMR spectrum of a grossular garnet containing 3.6 wt% H_2O.

Discussion

Although MAS-NMR spectra are often discussed solely in terms of isotropic chemical shifts, in the present study several other aspects are crucial from both methodological and interpretative standpoints. Therefore, in this section we will discuss first the conditions necessary for achieving line narrowing in high-speed ^1H MAS-NMR spectra. We will then discuss the diagnostic significance of the following spectroscopic parameters: the line widths of the ^1H MAS-NMR centerbands and their dependencies on field strength and spinning speed, the spinning sideband intensity patterns, and the isotropic chemical shift values. We will show in detail how these parameters can be used to distinguish between hydrogen species with different structural and dynamical characteristics. Finally, we will discuss information obtained about the structure and dynamics of nonstoichiometric hydrogen in the various minerals studied here.

Effectiveness of High-Speed Magic-Angle Spinning in Narrowing Solid-State ^1H NMR Spectra. The nonspinning ("wideline") ^1H NMR spectra of compounds containing hydrous species are influenced by the homonuclear (H-H) dipolar interactions as well as the heteronuclear dipolar couplings and chemical shift anisotropies. Broad spectra from polycrystalline compounds are the usual result. As pointed out earlier, the ability of magic angle spinning to narrow these broad resonances should depend mainly on the strength of the H-H dipolar interactions relative to the spinning speed. Since the dipolar Hamiltonian is proportional to r^{-3}, the inverse cube of the H-H distance, the effectiveness of magic angle spinning in narrowing ^1H NMR spectra of solids should be related to the interproton distances (and angles) in the crystal structure. Because precise proton positions have not been established for many of the compounds studied here, we use instead the density of the hydrogen atoms in the crystal lattice as a crude index of the strength of the homonuclear dipolar interactions. This density is expressed by the parameter C_H, the number of hydrogen atoms per unit volume, which is calculated from the unit cell volumes[11] and listed in Table I for the compounds under study. This approach is certainly an oversimplification, since it ignores the possibilities of pairing and clustering of hydrogen atoms. Nevertheless, our experimental results indicate that high-resolution ^1H MAS-NMR spectra with half-height line widths less than ca. 1.5 kHz (at 200 MHz) can be obtained at spinning speeds of 7–8 kHz if C_H is 15 atoms/nm^3 or less. For diaspore (AlOOH), for which C_H = 33.9 atoms/nm^3, no line-narrowing is observed. In contrast, substantial line narrowing is observed for gypsum ($CaSO_4 \cdot 2H_2O$), although C_H is very similar for this compound (32.4 atoms/nm^3). This difference in behavior between hydroxyl- and water-containing compounds arises from the inhomogeneous character of the H-H interactions within pairs of spins in molecular water, as discussed later.

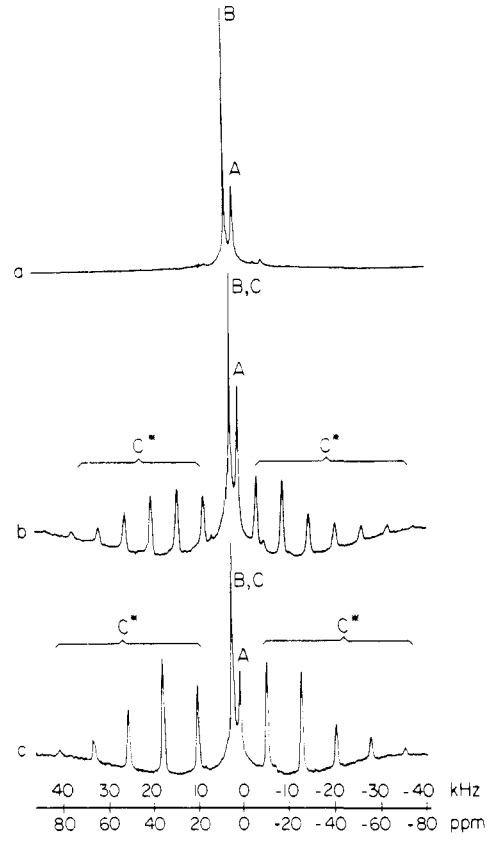

Figure 7. ^1H MAS-NMR spectra at 500.13 MHz of feldspars from three different localities. Three distinguishable species are labeled A, B, C; the spinning sidebands associated with C are indicated by C*: (a) Lake George, CO, spinning speed 6.2 kHz; (b) Elizabeth R Mine, spinning speed 4.7 kHz; (c) White Queen Mine, spinning speed 7.7 kHz.

Residual ^1H MAS-NMR Line Widths. Identification of the sources of residual ^1H MAS-NMR line widths is of interest not

(11) Wyckhoff, R. W. G. *Crystal Structures*; 2nd ed.; Interscience Publishers John Wiley and Sons: NY, London, Sydney, 1963.

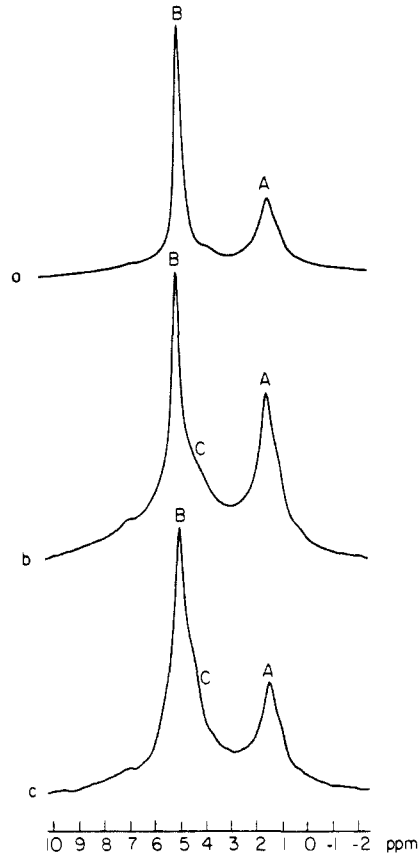

Figure 8. Expansion of Figure 7 about the centerband region.

only because they limit the achievable resolution but also because they may contain indirect structural information. The physical mechanisms responsible for the residual MAS–NMR line width can be elucidated by measuring line widths as a function of both spinning speed and field strength. The decrease in line width with increased spinning speeds observed for datolite and pyrophyllite (Figure 2) is the type of behavior expected when (homogeneous) homonuclear dipolar couplings contribute to the line width: for interactions which are entirely inhomogeneous in character, the line width would be independent of the spinning speed.

To use the field dependence of the line widths as a diagnostic tool, comparable spinning speeds must be employed. Three possible forms of the field dependence at constant spinning speed are schematically illustrated in Figure 13. (Since such data are obtained by using different NMR probes in different magnets, care must be taken to reduce the effects of magnetic field inhomogeneities and missetting of the magic angle.) One limiting case, where the ratio of the line widths in Hz equals the ratio of the respective field strengths (curve "a" in Figure 13), is expected when the line width is dominated by a distribution of isotropic chemical shifts. This situation occurs in water-bearing albite and rhyolite glasses, which show a chemical shift dispersion based on a continuous distribution of hydrogen-bonding strengths.[12] Another limiting case is a field-independent line width (in Hz) (curve "b"), resulting when the line width is dominated by homogeneous interactions. Experimentally, this case is exemplified by the hydroxyl resonance in hydroxyapatite, which has a line width of 240 Hz at both 200 and 500 MHz.[13] Field-independent line widths are also expected for isotropically mobile species in the extreme narrowing limit. Such species are usually characterized by extremely sharp line widths, even at very low spinning speeds. In these cases the experimental line widths may be dominated by the magnetic field inhomogeneity. Finally, a *decrease* of the line width in Hz with increasing field strength (curve "c") could occur for protons with strong dipolar couplings to nuclei experiencing second-order quadrupolar interactions (e.g., ^{27}Al).[14] These dipolar couplings are incompletely averaged by MAS, since the quantization axis of the quadrupolar nucleus is tilted from the magnetic field direction. The magnitude of this tilt, and the resultant broadening, increases with decreasing field strength.

For all of the compounds where line widths are reported at two field strengths in Table I except pyrophyllite and pectolite, the

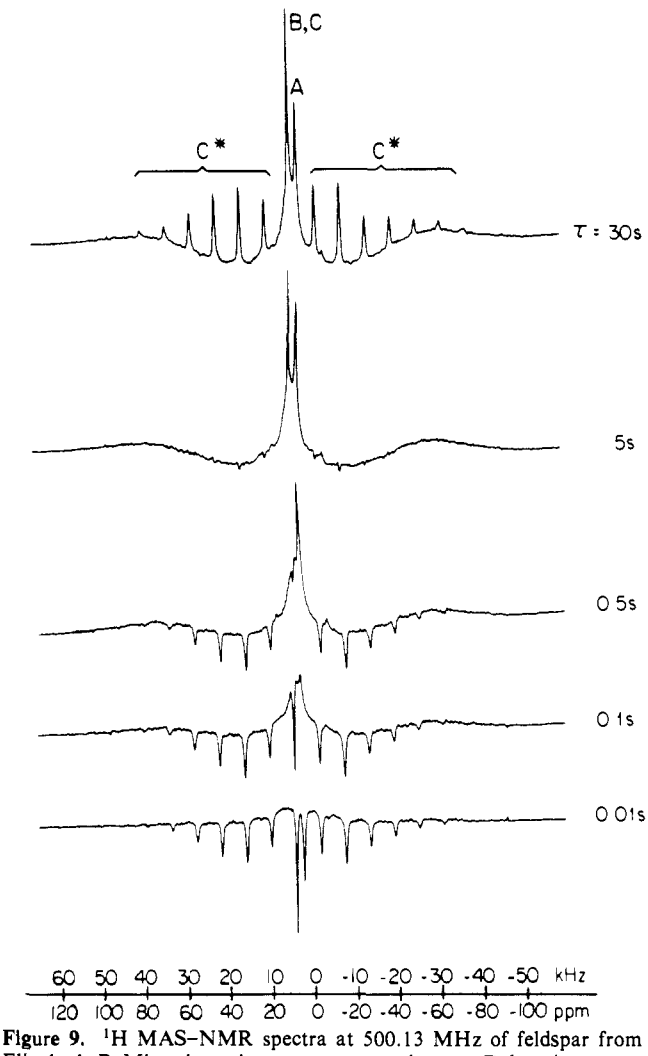

Figure 9. ^1H MAS–NMR spectra at 500.13 MHz of feldspar from Elizabeth R Mine, inversion-recovery experiment. Delay times τ as indicated.

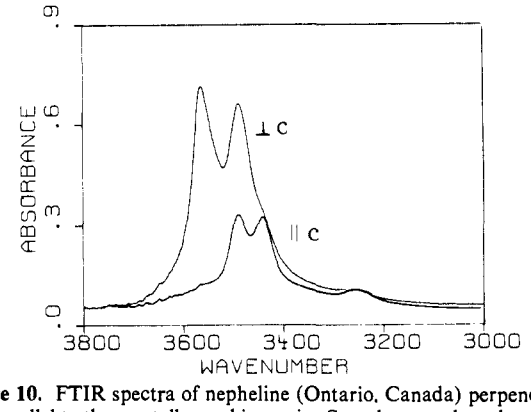

Figure 10. FTIR spectra of nepheline (Ontario, Canada) perpendicular and parallel to the crystallographic *c* axis. Sample was selected to be free of fluid inclusions.

(12) Eckert, H.; Yesinowski, J. P.; Silver, L. A.; Stolper, E. M. *J. Phys. Chem.*, in press.

(13) Arends, J.; Christoffersen, J.; Christoffersen, M. R.; Eckert, H.; Fowler, B. O.; Heughebaert, J. C.; Nancollas, G. H.; Yesinowski, J. P.; Zawacki, S. J. *J. Cryst. Growth* **1987**, *84*, 515.

(14) Menger, E. M.; Veeman, W. S. *J. Magn. Reson.* **1982**, *46*, 257.

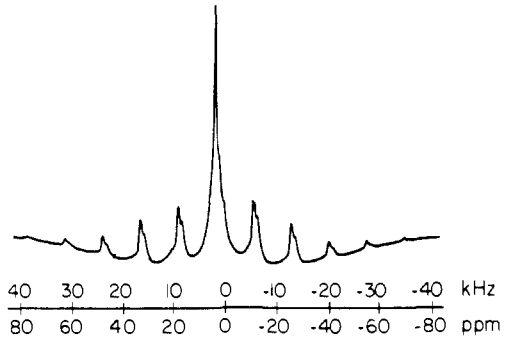

Figure 11. ^{1}H MAS-NMR spectrum at 500.13 MHz of nepheline, spinning speed 7.4 kHz.

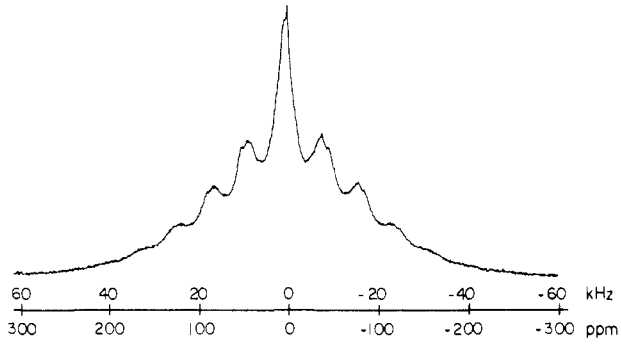

Figure 12. ^{1}H MAS-NMR spectrum at 200.27 MHz of grossular garnet, spinning speed 7.7 kHz.

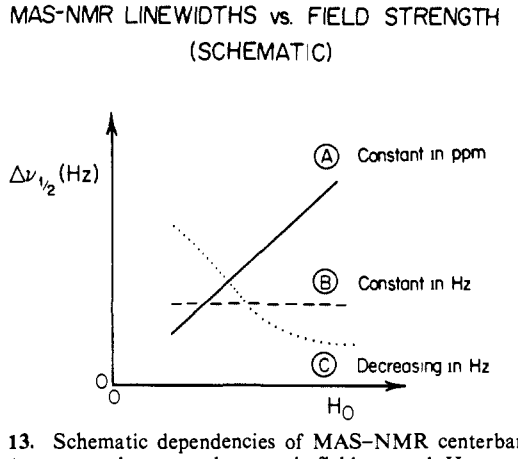

Figure 13. Schematic dependencies of MAS-NMR centerband line widths $\Delta\nu_{1/2}$ upon the external magnetic field strength H_0.

observed field dependence lies between curves "a" and "b" of Figure 13. The important contribution of homogeneous dipolar interactions to the residual line widths is demonstrated in Figure 14, which shows an approximate correlation of the MAS centerband line width at 200 MHz with the average proton density C_H in the crystal lattice. If these were the only important interactions, the field dependence would follow curve "b". The observed increase in line widths with field strength could arise from unresolved peaks with different chemical shifts or from dipolar couplings between protons with noncoincident chemical shift tensors as discussed in the next section. For pyrophyllite, the slight decrease in line width observed at higher field suggests that the proton–aluminum dipolar coupling contributes to the line width, as discussed above. A similar effect is seen in pectolite (due to dipolar coupling to Na). While in both cases such behavior might be predicted from the known crystal structures,[15,16] the experimental observation of such a decrease in line width with increasing field strength in compounds with unknown hydrogen

(15) Hendricks, S. B. *Z. Krist.* **1938**, *99*, 264. Gruner, J. W. *Z. Krist.* **1934**, *88*, 412. Wardle, R.; Brindley, G. W. *Am. Mineral.* **1972**, *57*, 732.
(16) Takeuchi, Y.; Kudoh, Y.; Yamanaka, T. *Z. Krist.* **1977**, *146*, 281.

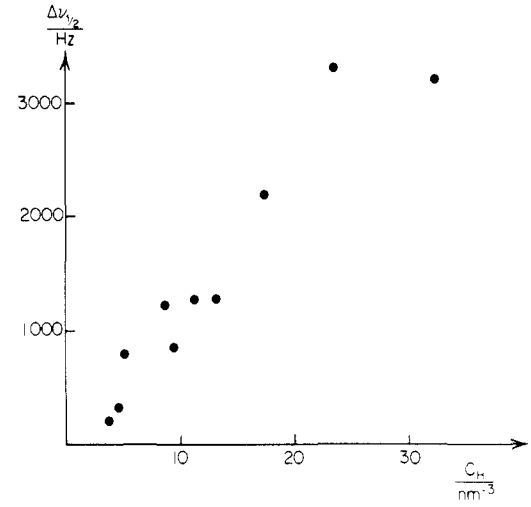

Figure 14. 200.27 MHz ^{1}H MAS-NMR center peak half-height linewidth $\Delta\nu_{1/2}$ versus average hydrogen density C_H, see text. Included are all compounds shown in Table I, as well as hydroxyapatite (C_H = 3.8 atoms/nm^3; $\Delta\nu_{1/2}$ = 240 Hz).

environments could be used to reveal the spatial proximity of protons to quadrupolar nuclei such as aluminum and sodium.

Finally, the empirical correlation in Figure 14 can be used to infer the presence of clustering of hydrogen atoms, if the experimental line width is much larger than the line width predicted from the average hydrogen density and if other sources of line broadening have been ruled out by field dependent measurements. This situation occurs in the grossular garnet discussed below.

MAS-NMR Spinning Sideband Intensities. The spinning sideband patterns observed in Figure 1 for minerals containing OH groups are governed by homo- and heteronuclear dipolar couplings and the ^{1}H chemical shift anisotropy. In contrast, the spectra of analcite and gypsum (Figures 3 and 4) have the spectral appearance expected for a homonuclear "Pake doublet"[17] in the slow spinning limit. This behavior has been predicted earlier on the basis of the inhomogeneous character of the dipolar interaction in isolated homonuclear two-spin systems.[5] In principle, the two hydrogen atoms of a water molecule in crystal hydrates cannot be simply viewed as such a two-spin system, since in addition to the intramolecular H–H interactions there are also sizeable intermolecular dipolar interactions with neighboring water molecules which render the total dipolar interaction homogeneous. However, Figures 3 and 4 demonstrate experimentally that fast magic angle spinning (ca. 8 kHz) can overcome this latter homogeneous interaction, resulting in spinning sideband patterns which closely resemble those expected for isolated water molecules.

The homonuclear dipolar coupling in an isolated two-spin system is inhomogeneous in the MAS-NMR sense only when the two spins have equal chemical shift tensors with identical orientations. When these orientations are different, as is the case for rigid isolated water molecules, complicated "powder pattern" line shapes are expected for the central MAS-NMR peak.[5] Since the chemical shift anisotropy of water molecules is sizeable (ca. 10 kHz at 11.7 T),[18] the resulting line shapes could be rather broad (an exact prediction of these effects requires detailed simulations). On the other hand, it is known that at room temperature the water molecules in many crystal hydrates, including gypsum, undergo twofold rotations about the bisector axis (180° "flips") which are fast on the NMR time scale (10^{-5} s).[19] This process results in identical averaged chemical shift tensors for the two protons and removes the complication mentioned above. Furthermore, such flips are effective in reducing the intermolecular dipolar couplings and hence facilitate averaging by magic angle spinning. It is

(17) Pake, G. E. *J. Chem. Phys.* **1948**, *16*, 327.
(18) Haeberlen, U. *High Resolution NMR in Solids*; Academic Press: New York, San Francisco, London, 1976; p 149.
(19) McKnett, C. L.; Dybowski, C. R.; Vaughan, R. W. *J. Chem. Phys.* **1975**, *63*, 4578.

therefore expected that the resolution observed in room temperature spectra for the hydrate water molecules in gypsum, analcite, and the nonstoichiometric samples discussed below may decrease at lower temperatures due to the "freezing out" of such flips.

Although the spectra of analcite (Figure 3) and gypsum (Figure 4) exhibit a similar dipolar sideband structure, some important differences warrant further discussion. The high resolution observed in the analcite spectrum, even at low spinning speeds, suggests that the water molecules are well-isolated (their precise location is uncertain because of statistical disorder of both sodium atoms and water molecules in the structure and the existence of noncubic forms[20,21]). In addition, the overall width of the analcite spectrum is less than that of gypsum. This observation accords with the results of a single-crystal ^{1}H NMR study of analcite,[22] which showed that the Pake doublet at room temperature has about a 20% smaller splitting than that at 77 K. This reduction was attributed to a low barrier to librational motions due to the absence of strong hydrogen bonding. The water molecule was described in this study as resembling that in clathrate compounds or in beryls and was suggested to have static rather than dynamic disorder.

It should be pointed out that spinning sideband patterns extending over a wide range of frequencies can also arise from dipolar interactions with unpaired electron spins localized on paramagnetic metal ions.[23] The presence of such an effect must be considered for naturally occurring samples, which often contain paramagnetic impurities. In contrast to the sidebands created by homonuclear H–H pair interactions, which are independent of the external field strength, spinning sideband patterns arising from interactions with paramagnetic spins should exhibit a strong field dependence. The total spectral width over which such sideband patterns extend should increase linearly with the magnetic field strength[23] and in addition should vary with the inverse temperature. In our studies at 200 and 500 MHz, paramagnetic ions do not appear to contribute significantly to the observed sideband intensities.

Figures 1–4 suggest that in a sample containing both OH and H_2O these species could be distinguished by their MAS–NMR sideband intensity patterns. Indeed, the analysis of sideband intensities has yielded speciation results in glasses that agree well with IR results.[12] However, for this approach to be successful these species must be sufficiently isolated (the spinning speed should exceed the intermolecular dipolar couplings). Furthermore, no molecular motions that modify the dipolar sideband pattern of H_2O should be present. The consequences of failure to meet these conditions are illustrated in the spectra of hemimorphite and lawsonite shown in Figure 5. In both cases the signal areas arising from the OH and the H_2O groups should be equal according to the sample stoichiometries, yet the relative sideband intensities in the two spectra are quite different. In lawsonite two OH groups are close to a water molecule (H–H distance = 200 pm),[24,25] an arrangement which leads to a strongly coupled four-spin system. In this situation, NMR transitions cannot be simply assigned to either OH or H_2O groups but rather involve combinations of spin states from both groups. At present, no theoretical simulations of sideband intensities from groups of homonuclear spins have been carried out. A similar situation applies in hemimorphite, where the water and hydroxyl groups form an infinite column in the structure, resulting in large dipolar couplings between the groups.[26] The sidebands extend over a range of only about 60 kHz, considerably less than the range observed in analcite and gypsum (Figures 3 and 4). Molecular motion of the water groups may be responsible for this reduction in width; indeed, a neutron diffraction study of hemimorphite revealed large thermal ellipsoids for the water hydrogen atoms that were attributed to positional disorder.[26]

Isotropic Chemical Shifts and Hydrogen Bonding. Experimental data[7] and theoretical calculations[27] indicate that the ^{1}H isotropic chemical shifts (δ_{iso}) of oxygen-bound hydrogen depend linearly on the O–H···O distance, an index of the hydrogen-bonding strength. A linear regression fit to all data available in the literature,[7,13,28–30] excluding early single-crystal multiple-pulse data, which have proven less accurate, yields the relationship[12]

$$\delta_{iso}\ (\text{ppm}) = 79.05 - 0.255\ d(\text{O–H···O})\ (\text{pm}) \qquad (1)$$

Although the crystal structures of the minerals in the present investigation have been obtained by diffraction methods,[20,21,24–26,31–43] it has often been impossible to obtain precise hydrogen positions in these studies. Table I lists estimates of the O–H···O distances obtained from the measured proton chemical shifts by using eq 1. For comparison, the corresponding distances derived from diffraction data are included where available. Apart from pectolite, the long O–H···O distances for all of the other compounds reflect rather weak hydrogen bonding. In this region the NMR-derived O–H···O distances must be viewed with some caution, since the linear regression leading to eq 1 includes very few distances larger than 290 pm. Indeed, the estimated distance of 298 pm for analcite disagrees with the interpretation of neutron diffraction data, which suggests the closest such distance to be 341 pm.[21] Nevertheless, ^{1}H MAS–NMR chemical shifts are able to reveal subtle differences corresponding to different hydrogen-bonding environments in minerals with nonstoichiometric hydrogen contents, as discussed below.

Application of ^{1}H MAS–NMR to Minerals Containing Nonstoichiometric Hydrogen: Feldspars. Recently infrared spectroscopic studies have identified water as a trace component in many feldspars.[44,45] As an example, Figures 6a–c show the infrared spectra of feldspars from three different localities. Analyses of these spectra indicate that water is present in two structurally bound forms (bands between 3630 and 3450 cm^{-1}) as well as in fluid inclusions (broad bands centered near 3420 cm^{-1}).[45] The proportion of the structural water component decreases from top to bottom in Figure 6; however, the absence of reliable extinction coefficients precludes a quantitative determination.

The ^{1}H MAS–NMR spectra (Figures 7–9) show three distinct forms of hydrogen giving rise to the resonances labeled A, B, and C, which are common to all samples but whose relative amounts vary. The peak at 1.5 ppm (resonance A) is assigned to an organic contaminant, since it is greatly diminished in the samples refluxed

(20) Mazzi, F.; Galli, E. *Am. Mineral.* **1978**, *63*, 448.
(21) Ferraris, G.; Jones, D. W.; Yerkess, J. *Z. Krist.* **1971**, *135*, 15.
(22) Ivleva, L. V.; Vakhrameev, A. M.; Gabuda, S. P. *Zh. Strukt. Khim.* **1973**, *14*, 44.
(23) Nayeem, A.; Yesinowski, J. P., to be published.
(24) Labotka, T. C.; Rossman, G. R. *Am. Mineral.* **1974**, *59*, 799.
(25) Baur, W. H. *Am. Mineral.* **1978**, *63*, 311.
(26) Hill, R. J.; Gibbs, G. V.; Craig, J. R.; Ross, F. K.; Williams, J. M. *Z. Krist.* **1977**, *146*, 241.
(27) Rohlfing, C. M.; Allen, L. C.; Ditchfield, R. *J. Chem. Phys.* **1983**, *79*, 4958.
(28) Scheler, G.; Haubenreisser, U.; Rosenberger, H. *J. Magn. Reson.* **1981**, *44*, 134.
(29) Rosenberger, H.; Grimmer, A. R. *Z. Anorg. Allg. Chem.* **1979**, *448*, 11.
(30) Ratcliffe, C. I.; Ripmeester, J. A.; Tse, J. S. *Chem. Phys. Lett.* **1985**, *120*, 427.
(31) Clark, J. R.; Appleman, D. E.; Christ, C. L. *J. Inorg. Nucl. Chem.* **1964**, *26*, 73.
(32) Perdikatsis, B.; Burtzlaff, H. *Z. Krist.* **1981**, *156*, 177.
(33) Donnay, G.; Barton, R. *Tschermaks Mineral. Petrogr. Mitt.* **1972**, *18*, 273.
(34) Hawthorne, F. C.; Grundy, H. D. *Can. Mineral.* **1976**, *14*, 334.
(35) Foit, F. F.; Phillips, M. W.; Gibbs, G. V. *Am. Mineral.* **1973**, *58*, 909.
(36) DalNegro, A.; DePieri, R.; Quareni, S.; Taylor, W. H. *Acta Crystallogr., Sect. B: Struct. Crystallogr. Cryst. Chem.* **1978**, *B34*, 2699, 3843.
(37) Dollase, W. A. *Z. Krist.* **1970**, *132*, 27.
(38) Foreman, N.; Peacor, D. R. *Z. Krist.* **1970**, *132*, 45.
(39) Busing, W. R.; Levy, H. A. *Acta Crystallogr.* **1958**, *11*, 798.
(40) Cole, W. F.; Lancucki, C. J. *Acta. Crystallogr., Sect. B: Struct. Crystallogr. Cryst. Chem.* **1974**, *B30*, 921.
(41) Pedersen, B. F.; Semmingsen, D. *Acta Crystallogr., Sect. B: Struct. Crystallogr. Cryst. Chem.* **1982**, *B38*, 1074.
(42) Ribbe, P. H.; Gibbs, G. V. *Am. Mineral.* **1971**, *56*, 24.
(43) LePage, Y.; Donnay, G. *Acta Crystallogr., Sect. B: Struct. Crystallogr. Cryst. Chem.* **1976**, *B32*, 2456.
(44) Erd, R. C.; White, D. E.; Fahey, J. J.; Lee, D. E. *Am. Mineral* **1964**, *49*, 831.
(45) Hofmeister, A. M.; Rossman, G. R. *Am. Mineral.* **1985**, *70*, 794.

in CCl_4 and packed into rotors washed with hexane and handled with gloves.

Peak B is assigned to water in fluid inclusions on several grounds. Its sharpness down to very low spinning speeds (<1 kHz) and the absence of spinning sidebands are symptomatic of a highly mobile species undergoing isotropic reorientation. Furthermore, the chemical shift of peak B is in the range expected for liquid water. Lastly, the IR results would predict the relative amount of water in fluid inclusions to increase in the order (Figure 7) c, b, a, the exact trend observed for peak B.

The extensive, largely field independent spinning sideband pattern of peak C in Figure 7 closely resembles the characteristic dipolar sideband pattern of water molecules in analcite (Figure 3). On this basis we assign peak C to a structurally isolated H_2O group. This molecule may experience 180° flips as well as significant librational motion, but any molecular motion must be strongly anisotropic.

The relative percentages of components B and C obtained from peak integrations by using fits to Lorentzian peaks are listed in Table I, along with the total water contents determined by NMR. The results show that the ratio of structural water to fluid inclusion water can vary greatly in feldspars. Relating variations in water content to the different geological conditions under which these minerals form is a promising area for future quantitative NMR studies.

The inversion-recovery spectra in Figure 9 show that the spin-lattice relaxation times T_1 of peaks A (organic contaminant), B, and C are distinct and vary over nearly two orders of magnitude. Such behavior is not commonly observed in proton-containing solids, since rapid spin-diffusion mediated by homonuclear dipolar couplings usually results in a uniform spin-lattice relaxation time. In the present samples, the absence of spin-diffusion between structurally incorporated and fluid inclusion water is explained by the large size of the fluid inclusions on the atomic scale. Figure 9 demonstrates the usefulness of inversion-recovery experiments for the selective observation of individual components.

The narrow line width of peak C and its chemical shift indicate that the anisotropically constrained water molecules are structurally isolated rather than clustered and are in a well-defined site involving relatively weak hydrogen bonding. In contrast to the IR data, which show the presence of two types of structural water environments,[45] the NMR data yield no evidence for more than one type. Since the water quantitation by NMR agrees very well with the amount of water measured by H_2 manometry, we can rule out the presence of hydrogen species that do not undergo line-narrowing by MAS. The two water sites may be structurally very similar and thus indistinguishable by MAS-NMR.

Not all nonstoichiometric hydrogen in minerals is necessarily bonded to oxygen. The ammonium-containing feldspar buddingtonite yields a high-resolution ^1H MAS-NMR spectrum (not shown) with moderate sideband intensities and a chemical shift (Table I) in agreement with values measured for the ammonium ion in other compounds by ^1H MAS-NMR.[30] In view of the short H-H distances within this four-spin system, the observation of narrow line widths indicates averaging of the homonuclear dipolar couplings by molecular motion, presumably reorientation of the NH_4^+ groups.

Quartz. The 200.27 MHz ^1H MAS-NMR spectrum at 7.9 kHz (not shown) of quartz from Hot Springs, AR, resembles that of Figure 7A. A peak at 4.7 ppm remains sharp down to very low spinning speeds (ca. 1 kHz) and can be assigned to mobile water in fluid inclusions. (These inclusions are observable microscopically and are responsible for the turbid appearance of the sample.) No other hydrous species is detected in the ^1H MAS-NMR spectrum, in concordance with earlier IR studies.[46]

Nepheline. Infrared absorption in the O-H stretch region of nephelines reveals that this nominally anhydrous mineral can incorporate small amounts of "water".[47,48] Contrary to earlier views,[47] recent infrared results (Figure 10) indicate that there are at least two structurally distinct water molecules in nepheline.[49] The ^1H MAS-NMR spectrum in Figure 11 confirms this interpretation. Two spinning sideband patterns typical of isolated, structurally anisotropic H_2O groups with an intensity ratio of roughly 3:2 are observed with calculated centerband positions at 4.6 and 3.4 ppm, corresponding to O-H···O distances of 292 and 297 pm, respectively. Inversion-recovery spectra exhibit a null-point for both sideband patterns at a recovery time of ca. 5 s, similar to that observed for the feldspar in Figure 9. In addition, these experiments reveal a sharp line at 4.6 ppm which is superimposed upon the centerbands of the above peaks. This sharp peak is assigned to highly mobile water molecules found in fluid inclusions (the IR sample had been selected to be free of fluid inclusions).

Grossular Garnet. Grossular garnet has the ideal formula $Ca_3Al_2(SiO_4)_3$. Hydrogen has been demonstrated to be a common minor element in garnets. When present at high concentrations, it enters the garnet structure as the "hydrogarnet substitution", in which a cluster of four OH^- ions replaces a SiO_4^{4-}.[2,50,51] In the end-member compound $Ca_3Al_2(OH)_{12}$ each hydrogen is bonded to one of the four oxygens about the tetrahedral void and is ca. 125 pm away from the tetrahedron centroid.[2] This arrangement results in two H-H distances of 182 and 242 pm, leading to strong homonuclear dipolar couplings.[52]

Figure 12 shows the ^1H MAS-NMR spectrum at 200.27 MHz of powdered grossular garnet containing 3.6 wt% H_2O.[51] Even a 7.7 kHz spinning speed does not yield a well-resolved spectrum, although the average hydrogen density in this mineral is comparable to that of pyrophyllite (see Table I and Figure 1). The broad line widths cannot be attributed to a distribution of isotropic chemical shifts, since the range would be unreasonably large; furthermore, the ^1H MAS-NMR spectrum at 500 MHz (data not shown) exhibits a comparable line width (in Hz). Paramagnetic effects do not appear to be significant, since the spectral width of the sideband pattern is only slightly greater at the higher field. The source of the broad line widths observed at a spinning speed of 7.7 kHz must therefore be the strong homogeneous proton-proton dipolar couplings. These results provide further experimental evidence for the hydrogarnet substitution model discussed above. The poorly resolved spinning sideband pattern of Figure 12 shows some additional fine structure, which may reflect the noncoincidence of the individual proton chemical shift tensors,[5] whose effect is discussed above.

Summary

Our results demonstrate that high-resolution ^1H MAS-NMR spectra of hydrous minerals can be obtained by employing high spinning speeds (up to ca. 9 kHz). Alternative approaches to high-resolution ^1H MAS-NMR involve elimination of the homonuclear dipolar couplings by multiple-pulse methods[53] or isotopic dilution with deuterium.[54] These couplings are retained in the present approach and provide valuable structural and dynamical information. Half-height line widths less than 1.5 kHz at 200 MHz are observed for minerals with hydrogen densities less than ca. 15 atoms/nm^3, and the line widths are roughly proportional to the hydrogen density. An exception to this general rule occurs when the hydrogen atoms are clustered, as in the case of grossular garnet.

Structurally isolated H_2O groups in minerals yield sharp peaks with a characteristic dipolar sideband pattern extending over ca. 100 kHz, as a consequence of the inhomogeneous character of the strong homonuclear dipolar coupling within a water molecule. Such a pattern provides a valuable diagnostic for the presence

(46) Rossman, G. R.; Weis, D.; Wasserburg, G. J. *Geochim. Cosmochim. Acta* **1987**, *51*, 2325.
(47) Beran, A. *Tschermaks Mineral. Petrogr. Mitt.* **1974**, *21*, 299.
(48) Wilkins, R. W. T.; Sabine, W. *Am. Mineral.* **1972**, *58*, 508.
(49) Rossman, G. R.; Aines, R. D., in preparation.
(50) Tilley, C. E. *Trans. Geol. Soc., South Africa* **1957**, *60*, 15.
(51) Aines, R. D.; Rossman, G. R. *Am. Mineral.* **1984**, *69*, 1116.
(52) Cohen-Addad, C.; Ducros, P.; Bertaut, E. F. *Acta Crystallogr.* **1967**, *23*, 220.
(53) Gerstein, B. C.; Pembleton, R. G.; Wilson, R. C.; Ryan, L. M. *J. Chem. Phys.* **1977**, *66*, 361.
(54) Eckman, R. *J. Chem. Phys.* **1982**, *76*, 2767.

of anisotropically constrained water molecules. In contrast, isotropically mobile water in fluid inclusions gives rise to very sharp peaks lacking spinning sidebands.

The use of two magnetic field strengths for ^1H MAS–NMR studies provides useful information concerning the sources of the residual line widths. In general, improved spectral resolution is obtained at the higher field, albeit to a lesser extent than predicted from the ratio of the field strengths. The lack of strongly field dependent sideband patterns demonstrates that paramagnetic ions do not significantly affect the spectra of the samples investigated.

Measurement of the isotropic chemical shifts enables one to discriminate different environments of hydrous species, in some cases even within the same mineral. These shifts can be used to estimate the strength of hydrogen bonding, as expressed by the O–H···O distance. The chemical shift does not provide a reliable means of distinguishing OH from H_2O groups, since the hydrogen-bonding strengths of these species may be comparable. Such a distinction is more readily accomplished by comparing relative spinning sideband intensities: the extensive dipolar sideband pattern of isolated structural water molecules differs markedly from the less intense sidebands characteristic of isolated OH groups. However, in minerals that contain OH and H_2O groups in close proximity, strong homonuclear dipolar interactions render spectral discrimination of these species impossible.

Both relative and absolute quantitation of the various hydrous species in minerals can be readily accomplished by using a suitable standard such as pyrophyllite as a ^1H MAS–NMR intensity reference. In this fashion, water contents in minerals down to levels of about 0.1 wt % have been determined in the present study. Two experimental limitations to such quantitative analyses have been encountered so far. The first one applies to the relatively broad spectra observed for the clustered hydrogen atoms in hydrogarnets, where it has not proven possible to quantitate water present at levels of ca. 0.2 wt %. Higher spinning speeds, or multiple-pulse methods, should help overcome the difficulties associated with relatively broad MAS–NMR peaks. The second limitation arises from the presence of background signals from the probe and contaminants. To the extent that these problems can be overcome, the inherent sensitivity of high field ^1H MAS–NMR should enable detection of hydrous species at levels below 0.01 wt% H_2O. These and other improvements will greatly enhance the usefulness of ^1H MAS–NMR as a unique quantitative tool for the study of trace amounts of hydrous species in geology and materials science.

Acknowledgment. The NMR studies were conducted at the Southern California Regional NMR Facility, supported by NSF Grant 84-40137. We are also grateful to Chevron Oil Field Research Corp. for their financial support for a MAS–NMR probe. One of us (G.R.R.) acknowledges support by NSF grants EAR 86-18200 and EAR 83-13098.

Registry No. $AlSi_4O_{10}(OH)_2$, 12269-78-2; $Mg_3Si_4O_{10}(OH)_2$, 14807-96-6; $Ca_2Mg_5Si_8O_{22}(OH)_2$, 14567-73-8; $Al_2SiO_4[F_{0.98}(OH)_{0.02}]_2$, 1302-59-6; $Na(Li,Al)_3Al_6(BO_3)Si_6H_{18}(OH,F)_4$, 12197-81-8; $CaBSiO_4(OH)$, 1318-40-7; AlOOH, 14457-84-2; $NaCa_2Si_3O_8(OH)$, 13816-47-2; $NaAlSi_2O_6·H_2O$, 1318-10-1; $CaSO_4·2H_2O$, 13397-24-5; $CaB_3O_4(OH_3)·H_2O$, 1318-33-8; $Zn_4Si_2O_7(OH)_2·H_2O$, 12196-21-3; $CaAl_2Si_2O_7(OH)_2·H_2O$, 1318-81-6; $KAlSi_3O_8$, 12251-43-3; $(NH_4,K)AlSi_3O_8$, 12418-12-1; $(Na,K)AlSiO_4$, 1302-72-3; SiO_2, 14808-60-7; $Ca_3Al_2(SiO_4)_3$, 1302-57-4; HO, 3352-57-6.

Theoretical Study of α-Lactone, Acetoxyl Diradical, and the Gas-Phase Dissociation of the Chloroacetate Anion

Danko Antolovic, Vernon J. Shiner, and Ernest R. Davidson*

Contribution from the Department of Chemistry, Indiana University, Bloomington, Indiana 47405. *Received December 26, 1986*

Abstract: The influence of the α-carboxylate group on the mechanism and energetics of the departure of the chloride anion from chloroacetate was investigated theoretically for a gas-phase reaction. Ab initio Hartree–Fock and configuration-interaction methods were used to obtain the energy values along the reaction path, as well as a description of the intermediate states. Several basis sets were utilized and the results compared. It was found that the three-membered ring of the α-lactone closes simultaneously with the departure of the electrophile and that a loosely bound complex is formed in the process. Acetoxyl zwitterion and diradical were also investigated in detail. The zwitterion is high in energy. The diradical has many states that are similar to the isoelectronic trimethylene methane but with the symmetry instability problems found previously for formyloxyl.

In this paper we report a quantum chemical investigation of the mechanistic and energetic aspects of the gas-phase reaction (1). This reaction is a computationally accessible model, which

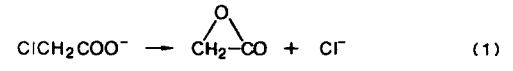

(1)

we investigate with the aim of shedding additional light on the role of the α-carboxylate group in nucleophilic substitution reactions. Our primary objective in this work was to determine whether the reaction follows an S_N1 or an internal S_N2 mechanism, i.e. whether the departure of the halogen and the closing of the ring constitute two separate events or a single, concerted process.

A second objective was to study in detail the acetoxyl diradical, which has many features in common with the isoelectronic trimethylenemethane and formyloxyl radicals. The acetoxyl radical has sometimes been described as a zwitterion so we have also investigated this possibility.

Nucleophilic Substitutions

The process observed in the laboratory was not the gas-phase reaction (1) but the nucleophilic substitution reaction in solution (eq 2). The main effects of the carboxylate group close to the

$$RCH(X)COO^- + Y^- \rightarrow RCH(Y)COO^- + X^- \quad (2)$$

substitution site consist of an increase in the reaction rate (relative to similar substitutions without the carboxylate) and the retention of stereochemical configuration at the substitution site.[1] The

(1) Cowdrey, W. A.; Hughes, E. D.; Ingold, C. K. *J. Chem. Soc.* **1937**, 1208; **1938**, 1243. Grunwald, E.; Winstein, S. *J. Am. Chem. Soc.* **1948**, *70*, 841.

0002-7863/88/1510-1375$01.50/0